Materials Science Forum Vols. 636-637 (2010) pp 865-873
Online available since 2010/Jan/12 at www.scientific.net

doi:10.4028/www.scientific.net/MSF.636-637.865

Advanced Multi-Metallic SOFC Anode Development by Mechanical Alloying Route

T.A.G. Restivo[1,a], D.W. Leite[2,b] and S.R.H. Mello-Castanho[1,c]

[1] Instituto de Pesquisas Energéticas e Nucleares – CCTM – IPEN – São Paulo – SP Brasil

[2] Instituto de Pesquisas e Estudos Industriais – IPEI - FEI - S. B. do Campo - SP Brasil

[a]guisard@dglnet.com.br, [b]dwill@fei.edu.br, [c]srmello@ipen.br

Keywords: Cermet, SOFC anode, Sintering kinetics, Mechanical alloying, SAS.

Abstract. Anodes composed of Ni-YSZ (yttria-stabilised zirconia) cermets are the key material to allow direct biofuel feeding to Solid Oxide Fuel Cell (SOFC) devices due to its internal reforming capability. The main challenge among these materials is related to carbon deposition poisoning effect when C-bearing fuels are feed. The work deals with these issues by alloying Ni with some metals like Cu to conform a multi-metallic anode material. Mechanical alloying (MA) at shaker mills is chosen as the route to incorporate the metal and ceramic powders in the anode material, also leading to better sintering behaviour. A projected cermet material is conceived where a third metal can be added based on two criteria: low Cu solubility and similar formation enthalpy of hydrides regarding Ni. Refractory metals like Nb, W and Mo, seems to fulfil these characteristics, as well as Ag. The MA resulted powder morphology is highly homogeneous showing nanometric interpolated metal lamellae. The sintering behaviour is investigated by conventional dilatometry as well as by stepwise isothermal dilatometry (SID) quasi-isothermal method to determine the sintering kinetic parameters. Based on these tools, it is found the Cu additive promotes sintering to obtain a denser anode and therefore allowing lower process temperatures. The consolidation is achieved through the sintering by activated surface (SAS) method allied to liquid phase sintering process, where the third metal additive also has influenced. The final cermet can be obtained at one sole process step, dispensing pore-forming additives and reduction treatments. The sintered microstructure demonstrates the material is homogeneous and possesses suitable percolation networks and pore structure for SOFC anode applications.

Introduction

Solid oxide fuel cells (SOFC) is one of the most promising technologies to take part at electrical energy generation systems wide world due to its high conversion efficiency, energy output and low pollutant release. The anode Ni-YSZ (yttria-stabilized zirconia) is the key SOFC component owing to its functions, including fuel oxidation, electronic conductivity and O^{2-} ion transport. Fossil and biologic fuels are admitted directly at the anode volume thanks to the steam reforming reactions and operation flexibility. SOFC technology is especially attractive for brazilian energetic matrix due to the actual structure for ethanol production and distribution. However, technical problems related to poisoning by carbon deposition at the anode still impart the full employment of such alcohol fuels. Low steam to fuel ratio turns the CO reforming product to reverse to carbon, which may be deposited and block the active sites and pores, degrading the anode performance [1]. The mechanisms of carbon deposition, which arise from fuel reforming and Boudouard reaction, involve C solving in Ni lattice and further precipitation as filaments that cover the metal surface and pores [2,3], reducing drastically the cell power output. While Cu additive is known to improve the carbon tolerance [4,5], the Ni-Cu alloy is easily formed, leading to electrocatalytic properties degradation in the Ni catalyst. Therefore it is imperative to free Cu into the precipitated state to meet these goals.

The conventional preparation route for Ni-YSZ anodes involves mixing YSZ and NiO ceramic powders followed by sintering in an oxidant atmosphere and reduction at 900-1000°C in a further process step or in situ by the fuel in the SOFC [1, 5, 6]. Since the shrinkage produced by the

reduction of NiO to Ni is rather small, pore-forming additives should be employed, like graphite, in order to reach a suitable porosity range for gas flow (nearly 35%) [6].

The mechanical alloying (MA) process is investigated in the present work as a mean to obtain directly the SOFC anode material from YSZ and metallic Ni powders, avoiding pore-forming aids and further reduction treatments. This method is also suitable in order to incorporate metallic powder additives [7], like Cu, as well as other metallic elements, even with different physicochemical properties. Successive alloying with refractory metals is performed to the Cu-Ni-YSZ anode material aiming to free Cu at the precipitated state due to Cu low solubility in the metals. As a collateral effect, the MA high energy milling is expected to promote densification through sintering by activated surface method (SAS), where active metallic and ceramic surfaces are created during milling operation and further during the heating cycle. The SAS concept foresees the increasing of the powder sinterability leading to anticipated contraction onset temperature [7,8]. The process concept based on MA ultimately drives the powder material into a project microstructure composed of thin metallic films layers coating the ceramic particles.

Besides conventional dilatometry, one important tool employed for evaluation of the powder sinterability is the stepwise isothermal dilatometry (SID) approach. The SID method is a quasi-isothermal analysis where the kinetic parameters can be determined in one sole experiment as a function of the temperature [9-13]. The analysis is accomplished by imposing several isotherms at the sintering temperature range during the heating cycle. Equationing begins with the basic shrinkage relation:

$$\Delta L/L_o = y = [K(T).t]^n \quad (1)$$

where K(T) is analogous to reaction rate constant and n is a parameter related to the mechanism, equivalent to reaction order. SID method is a differential kinetic one where the Eq. 1 is applied into the differential form:

$$dy/dt = K(T).f(y) \quad (2)$$

Assuming the sintering process as isotropic, the normalized volumetric shrinkage can be expressed as $Y = (V_o\text{-}V_t)/(V_o\text{-}V_f) = (L_o^3\text{-}L_t^3)/(L_o^3\text{-}L_f^3)$, where the subscriptions o, t and f mean the dimension values at the beginning, at a time t and at the end of the sintering. Replacing the relative linear shrinkage $\Delta L/Lo$ in the Eq.1 by the relative volumetric shrinkage $Y/(1\text{-}Y) = (V_o\text{-}V_t)/(V_t\text{-}V_f)$, followed by differentiation on time, a normalized shrinkage equation can be developed [13-14]:

$$dY/dt = nK(T)Y(1\text{-}Y)[(1\text{-}Y)/Y]^{1/n} \quad (3)$$

At each isotherm, the Plot $\ln\{(dY/dt)[1/Y(1\text{-}Y)]\}$ versus $\ln[(1\text{-}Y)/Y]$ yields a straight line from what n and K(T) are calculated. The rate constant parameter obeys the Arrhenius Equation:

$$K(T) = A.\exp(-Q/RT) \Rightarrow \ln[K(T)] = \ln A - Q/RT \quad (4)$$

Therefore, the apparent activation energy Q can be determined from the plot $\ln[K(T)] \times 1/T$.

Experimental

Starting powders were YSZ (cubic zirconia, 8mols%Y_2O_3, Tosoh Corp.), metallic Ni with 28µm average particle size (CIRQ Cromato, 400 mesh, 99,6 mass% purity) and a 3µm-Cu powder exceeding 99.9 mass% purity. One 3µm Ni powder 99,8% purity (mass base, Aldrich) was employed in some samples, while the refractory metals (Nb, W, Mo) had the same mean particle size and grade. All sample compositions were set at 40vol%metal-YSZ, previously mixed and submitted to high energy milling in shaker mills at a rotation speed of 10 and 19 Hz for 1 to 8-hour

periods. Ultra-high molecular weight (UHMW) polyethylene and PTFE vials were used with a milling medium of 5mm diameter tetragonal zirconia YTZ spheres. Another experimental set was performed employing vanadium hard steel (VC131) vial and 5mm diameter 52100 grade steel spheres. When the powders were alloyed with refractory metals, a milling sequence was used over 3-h period: YSZ+Ni, +Cu, +Me (refractory). The balls-to-powder mass ratio was 10:1 for a total powder mass of 10g. For purposes of comparison, two samples – 40vol%Ni-YSZ and 55vol%NiO-YSZ – were prepared by mixing and homogenizing the raw powders in alcohol slurries, and the former is referred to as homogenized cermet. MA was performed either in air or under argon and vacuum if reactive metals are included. The powder samples were pressed uniaxially at 150MPa to conform 7mm diameter pellets. The pellets were sintered under argon flowing gases both in a muffle furnace and in a vertical dilatometer/TMA (Setaram Labsys TMA 1400°C). The heating rate was 10°C/min up to 1250-1350°C and dwelling time of 1 hour. SID heating cycles used the same heating rate while several isotherms were programmed at each 50°C, from 200°C up to 1200°C. The TMA load for all experiments was set at 2g in order to cause no influence on sintering profiles and satisfy the isotropic assumption. One sample was analysed by simultaneous TGA/DTA up to 1200°C (Setaram Labsys TG/DTA 1600°C) to give more assertions regarding the phenomena talking place during sintering. The SAS process was carried out in a tubular furnace with 10% water vapour- argon flow up to 1200°C for 1h.

Results and Discussion

The Ni-YSZ powder microstructure is shown in Fig. 1 at SEM-BSE, prepared by impregnated technique following by polishing down to 1μm. One can see the typical lamellae MA structure that tends to be refined and totally homogeneous at higher milling times. The constituents Ni and YSZ are dispersed in both white and grey fields.

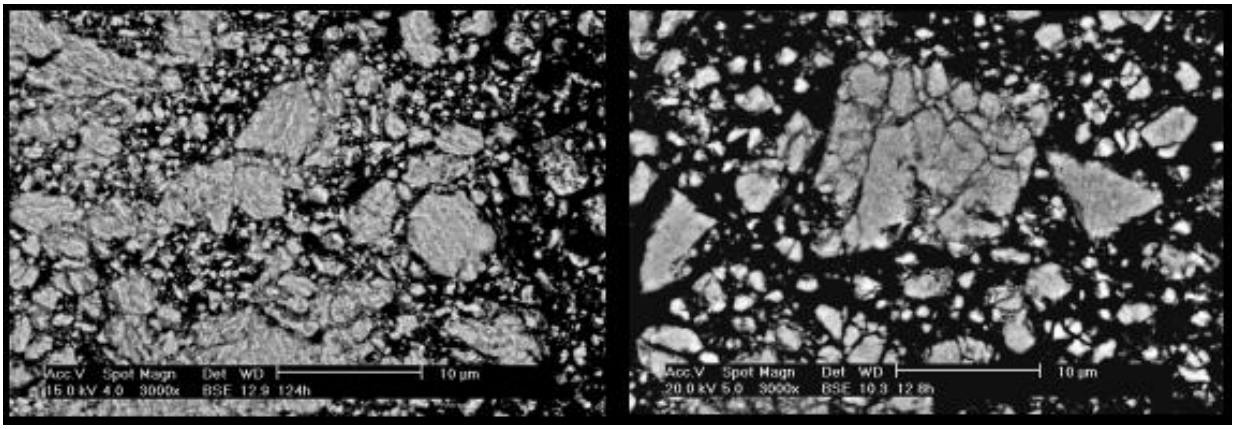

Fig. 1. Ni-YSZ MA powders: 4-h (left) and 8-h milling time.

A closer examination at the powder (Fig. 2) has demonstrated the projected structure has been achieved: YSZ small particles has been placed internally, plated by metallic films. Fig. 3 examines the Ni-YSZ powders with higher magnification by TEM. The Ni and YSZ atomic planes can be identified connected with small domain areas or superimposed, indicating high defect density. The ultimate particle size and grains are in the nanometric range.

Analysis by X-ray diffraction (Fig. 4) shows the main constituent Ni and YSZ preserves the original peaks, while they have underwent peak broadening due to increase of defects and reducing the crystallite size. Ni reflection peaks are broadened when Cu is added while the last own peaks are absent, indicating a Ni-Cu alloy has been formed during MA milling. The metal approaches the amorphous state as the milling time is increased.

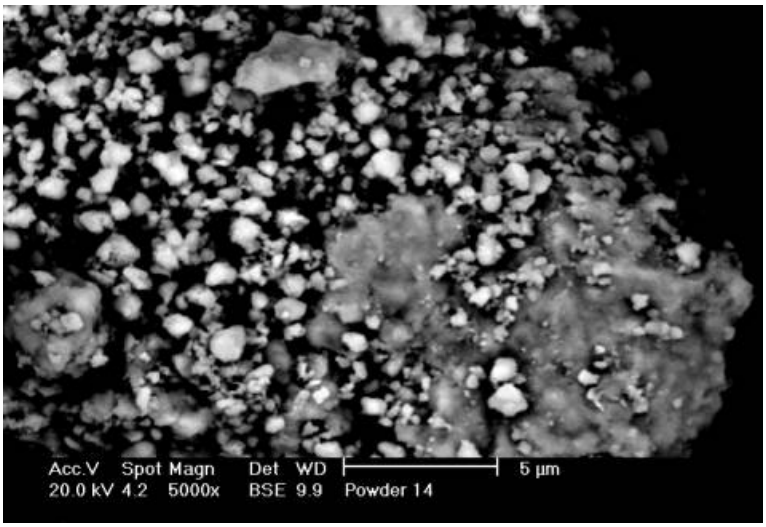

Fig. 2. SEM-BSE detail evidencing Ni plating of YSZ particles.

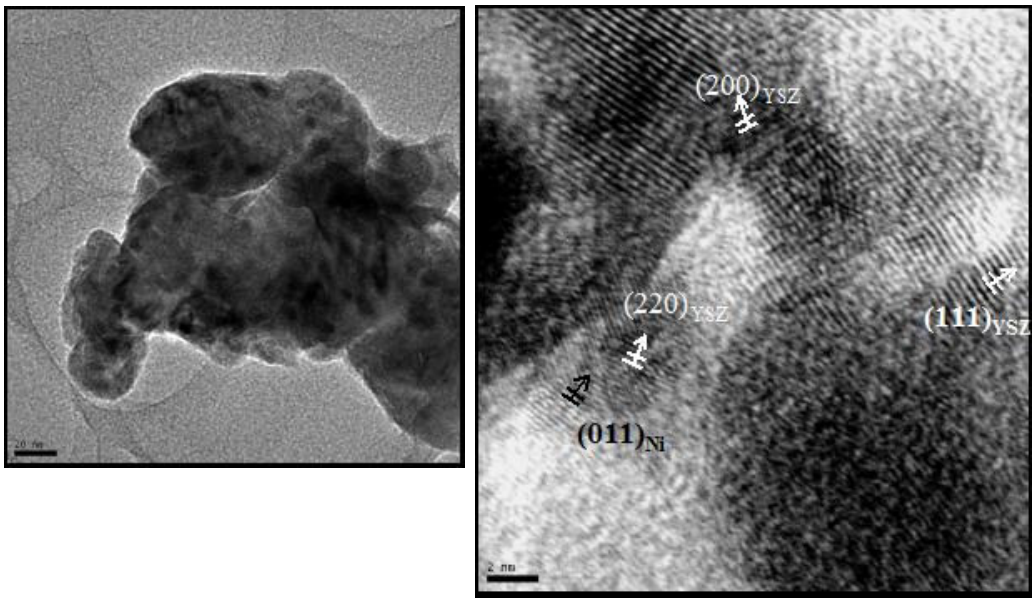

Fig. 3. TEM images showing Ni-YSZ dispersing at nanometric level.

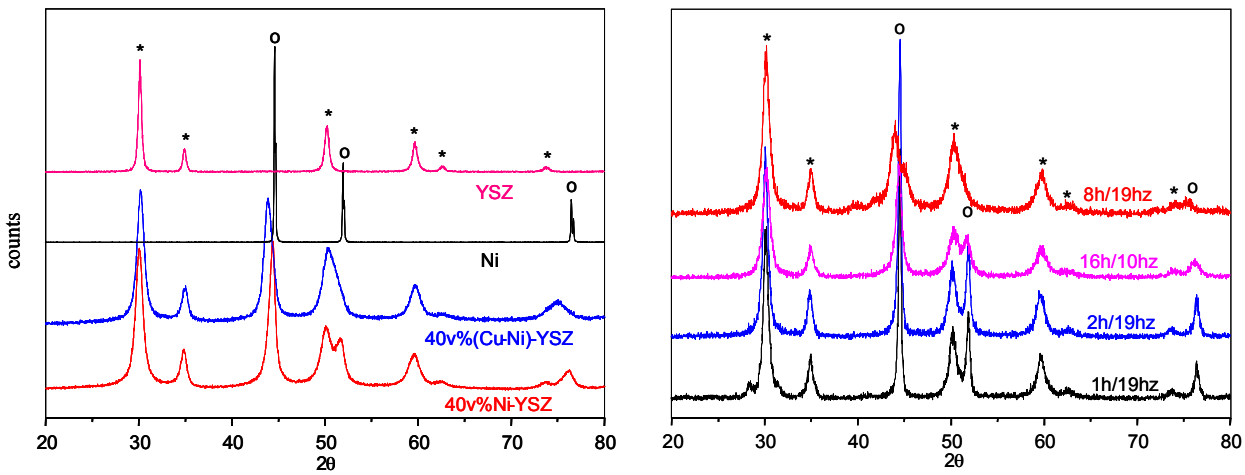

Fig. 4. X-ray profiles of MA powders (Cu-)Ni-YSZ; ° Ni ; * YSZ.

The sintering behaviour is influenced by the milling accordingly to dilatometric curves in Fig. 5. It has been assigned an initial sintering temperature of only 195°C for the most energetic milled sample (MA 8h). However, the total shrinkage is smaller for MA powders compared to the homogenized one. This fact is beneficial as SOFC anode preparation method once pore-forming additives are not required. The sintered densities of all (Cu-)Ni-YSZ samples lied in the range 65-73%TD, suitable for SOFC applications. Also, NiO-YSZ material densifies extensively compared to the MA cermets.

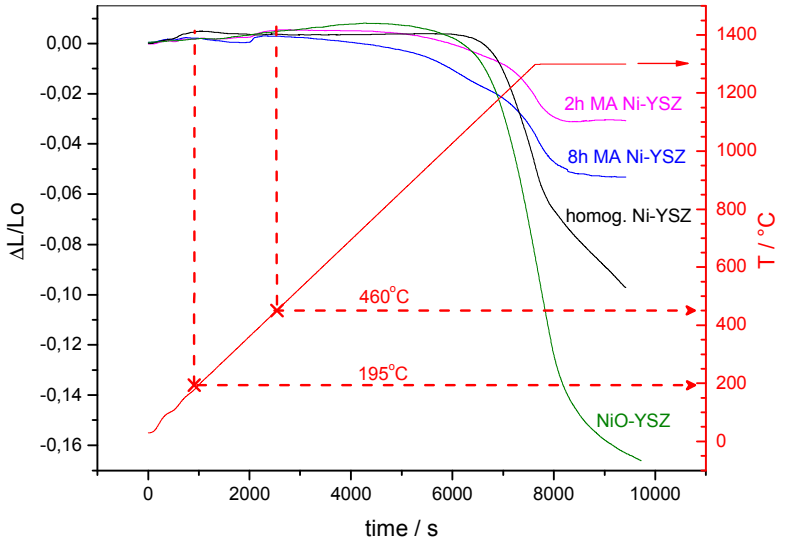

Fig. 5. Sintering curves for MA and homogenized 40vol% Ni-YSZ and NiO-YSZ.

Refractory metal additions to MA processed powders were successful to separate the Cu in the precipitated state from Ni as seen in Fig. 6. The Cu peak is clearly separated while the Ni one is less shifted to smaller 2θ angles. Original Ni and YSZ profiles are included to allow localizing each reflection. Accordingly to X-ray analysis (Fig. 7), some compounds were formed after sintering of MA powder pellets submitted to high energy transfer conditions, as a result of C contamination from the container: ZrC and $CuZrO_3$. The last has been found when Cu replaces part of Ni as well as a deposit in the sintering boat, indicating some vapour phase reaction product.

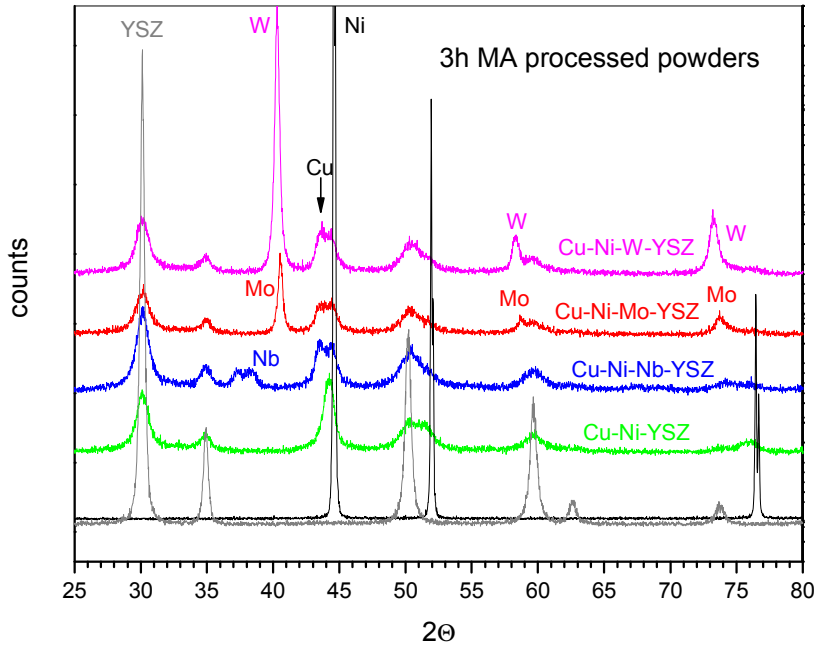

Fig. 6. X-ray profiles for 8vol% Me- 12vol% Cu- 20vol% Ni – YSZ; Me = W, Nb, Mo.

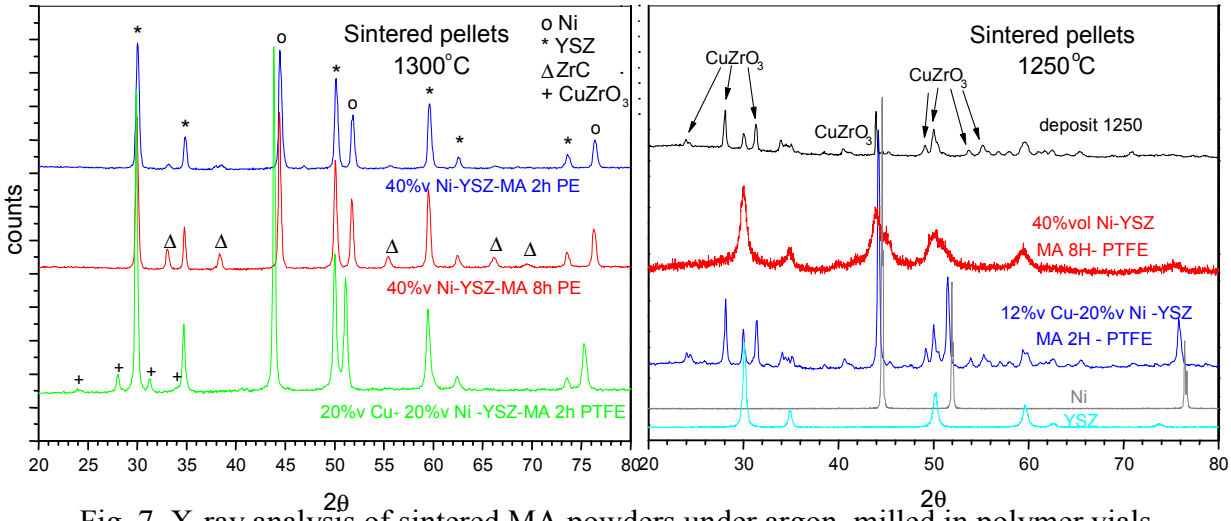

Fig. 7. X-ray analysis of sintered MA powders under argon, milled in polymer vials.

By the other side, the sintered MA 3h powder pellets X-ray profiles in Fig. 8, whose has been milled in steel vials, do not show ZrC precipitation. When Nb and Cu are alloyed, it still shows some $CuZrO_3$ suggesting Nb acts as a reducer for ZrO_2, leaving Cu to react. Ni peaks are further shifted due to refractory metals alloying while Cu peaks are not preserved. Lower sintering temperatures are required as well as increasing milling time to isolate Cu metal.

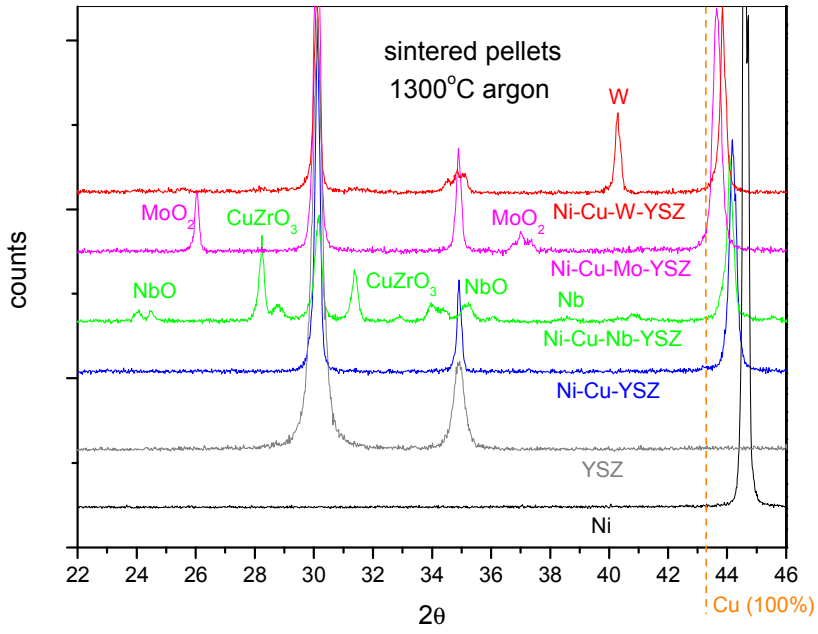

Fig. 8. X-ray profiles of sintered pellets milled by MA 3h.

Sintering Kinetics. Sintered kinetics as determined by SID method is shown in Figs. 9 and 10 for polymeric and steel vials. The apparent activation energies (Eact) for Cu added powders are much lower indicating this metal promotes sintering in an efficient way. The low melting point of Cu can lead to liquid phase formation, accelerating densification. Milling in steel vessels further increases the powder sinterability as seen by the activation energy values. One can divide the sintering process in 2 steps: metal sintering at low temperature with small Eact and YSZ sintering at higher temperatures at high Eact. It is confirmed the shrinkage of such powders starts at very low temperature, especially when Cu is alloyed. YSZ controls the kinetics from 750°C, which is substantially lower than normal contraction onset for zirconia (950°C). These results demonstrate

the MA process can improve the powder sinterability by incorporating powder additives in a proper way. Moreover, the carbon contamination imparts somewhat the densification (higher Eact) due to carbide phase formation blocking effect on the contact patterns.

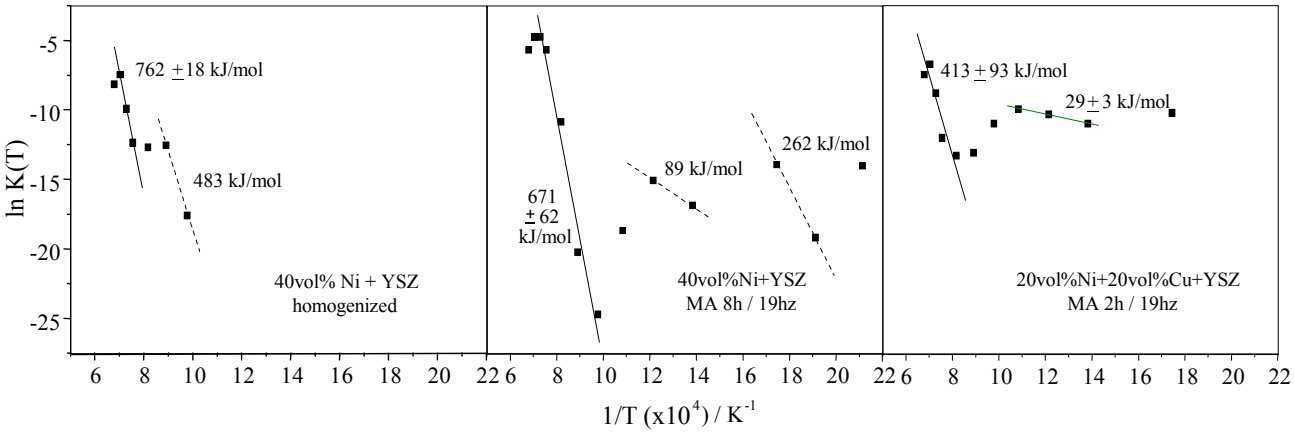

Fig. 9. Activation energies of sintering determined by SID method for homogenized and MA powder pellets up to 1200°C; polymer vials.

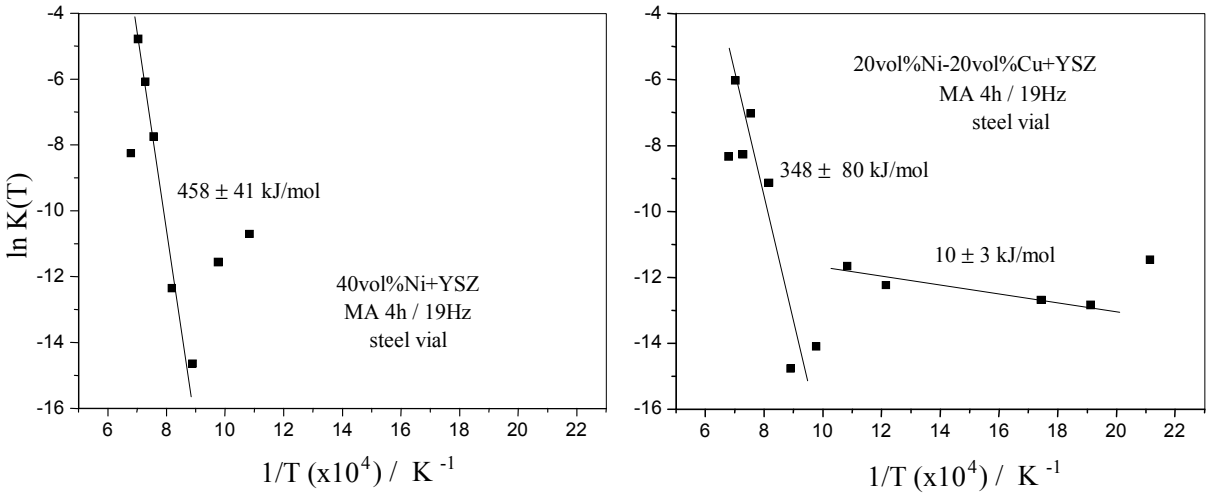

Fig. 10. Activation energies of sintering; steel vials.

Sintering by Activated Surface. The SAS conceptual process was tried for the very first time. Its principle involves plating ceramic particles by metal microforging in the MA process. The resulting thin film is adherent at a micrometer level, prone to fill the defects at ceramic surface and hence blocking surface diffusion. In some intermediate temperature during sintering heating cycle, the reactive refractory metal films can undergo partial oxidation at controlled oxygen potential. Some metal films like MoO_3 and WO_3, besides NiO, are volatile, therefore may leave the preserved ceramic surfaces to reactivate sintering. Table 1 shows the results of SAS process at 1200°C under argon-10% water vapour. The powder pellets composed of Cu-Ni-YSZ has attained a similar sintered density by SAS at 1200°C compared to conventional sintering at 1300°C. The same tendency can be approached for Mo-bearing sample at 1200°C SAS process. As the weight gain (Δm) is higher for the more reactive refractory metal additive, the sintered density is lowered. This fact indicates the oxygen potential is excessive for some metals like W and Nb, but suitable for Ni and Mo.

Table 1. SAS process results; comparison between sintered densities (%TD) at SAS and conventional sintering processes; Δm is the mass variation after sintering.

sample	Time [h]/ hz	vial	T [°C]	Δm [%]	Green dens.	Sint. Dens.
20v%Ni-12v%Cu-8v%Nb-YSZ	3 / 19	steel	1300	+0,42	57,83	72,29
20v%Ni-12v%Cu-8v%Nb-YSZ SAS	3 / 19	steel	1200	+1,33	58,22	65,13
20v%Ni-12v%Cu-8v%Mo-YSZ	3 / 19	steel	1300	-0,97	57,31	65,95
20v%Ni-12v%Cu-8v%Mo-YSZ SAS	3 / 19	steel	1200	+0,39	57,71	63,24
20v%Ni-12v%Cu-8v%W-YSZ	3 / 19	steel	1300	-1,48	57,23	81,50
20v%Ni-12v%Cu-8v%W-YSZ SAS	3 / 19	steel	1200	+0,85	57,87	71,92
12v%Cu-28v%Ni-YSZ	4 / 19	stell	1300	-2,71	54,10	76,91
12v%Cu-28v%Ni-YSZ SAS	4 / 19	steel	1200	-2,84	56,19	76,86

Conclusions

Mechanical alloying processing is a suitable method for preparing SOFC anode powder materials, leading to higher shrinkages of compacts at lower temperatures while maintaining the required porosity and good homogeneity. The powder morphologies can be tailored to a projected microstructure where thin metal films cover the ceramic particles, which become internal. Cu additions can be liberated at the powder after MA milling by means of alloying of some third metals whose repulse the former. Sintering kinetics analysis of Cu-Ni-YSZ pellets demonstrates the process take place by 2 steps: metal sintering at low temperature followed by ceramic control from 750°C. The new SAS process concept is promised as long as the sintering temperature can be additionally lowered by 100°C for Cu-Ni-YSZ and Mo-Cu-Ni-YSZ.

Acknowledgements

The authors express thanks to Brazilian research funding agencies FAPESP, FINEP-MCT and CNPq for their financial support of this work.

References

[1] N.Q. Minh, J. Am. Ceramic Soc. Vol. 76 [3] (1993), p. 563-88

[2] Atkinson et al. Nature Materials, Vol 3, Issue 1, jan 2004, 17-27

[3] J. Macet, B. Novosel, M. J. Mannsek. European Ceram. Soc. Vol. 27 (2007), p. 487-91

[4] C. Sun, U. J. Stimming. Power Sources (2007), oi:10.1016/j.jpowsour.2007.06.086

[5] M.D. Gross, J.M. Vohs, R.J. Gorte. Electrochimica Acta, Vol. 52 (5) (2007), p. 1951-57

[6] J. Sankar, Z. Xu, S. Yarmolenko, FY 2005 Progress Report for Heavy Vehicle Propulsion Materials, 4D. Processing and Characterization of Structural and Functional Materials for Heavy-Vehicle Applications, 89-97, (may 2006)

[7] T.A. Guisard Restivo, S.R.H. Mello-Castanho. Materials Science Forum Vols. 591-593 (2008), p. 514-520

[8] T.A.G. Restivo, S.R.H. Mello-Castanho. Journal of Power Sources Vol. 185 (2008), p. 1262–1266

[9] O. T. Sorensen. J. Thermal Analysis, vol. 38 (1992) 213-228

[10] P. L. Husum, O. T. Sorensen. Thermochimica Acta, Vol.114 (1987), P. 131-138

[11] C. C. Guedes E Silva, F.M.S. Carvalho, T. A. G. Restivo. Estudo dos Mecanismos de Difusão em Cerâmicas a Base de Alumina. In: 14ª Congresso Brasileiro de Ciência e Engenharia de Materiais, Águas de São Pedro, SP, Brasil (2000)

[12] T.A.G. Restivo, L. Pagano Jr. Sintering studies on the $UO_2.Gd_2O_3$ system using SID method, In: Conference on Characterization And Quality Control Of Nuclear Fuels 2002, Hyderabad, India (2003)

[13] T.A.G. Restivo, L. Pagano Jr. Effect Of Additives On The Sintering Kinetics Of The $UO_2.Gd_2O_3$ System, In: TCM Brussels, (2003)

[14] M. El Sayed Ali, O.T. Sorensen. Riso-R-518 (1985), p. 12

Advanced Materials Forum V
doi:10.4028/www.scientific.net/MSF.636-637

Advanced Multi-Metallic SOFC Anode Development by Mechanical Alloying Route
doi:10.4028/www.scientific.net/MSF.636-637.865

References

[1] N.Q. Minh, J. Am. Ceramic Soc. Vol. 76 [3] (1993), p. 563-88
doi:10.1111/j.1151-2916.1993.tb03645.x

[2] Atkinson et al. Nature Materials, Vol 3, Issue 1, jan 2004, 17-27
doi:10.1038/nmat1040
PMid:14704781

[3] J. Macet, B. Novosel, M. J. Mannsek. European Ceram. Soc. Vol. 27 (2007), p. 487-91
doi:10.1016/j.jeurceramsoc.2006.04.107

[4] C. Sun, U. J. Stimming. Power Sources (2007), oi:10.1016/j.jpowsour.2007.06.086

[5] M.D. Gross, J.M. Vohs, R.J. Gorte. Electrochimica Acta, Vol. 52 (5) (2007), p. 1951-57
doi:10.1016/j.electacta.2006.08.005

[6] J. Sankar, Z. Xu, S. Yarmolenko, FY 2005 Progress Report for Heavy Vehicle Propulsion Materials, 4D. Processing and Characterization of Structural and Functional Materials for Heavy-Vehicle Applications, 89-97, (may 2006)

[7] T.A. Guisard Restivo, S.R.H. Mello-Castanho. Materials Science Forum Vols. 591-593 (2008), p. 514-520
doi:10.4028/www.scientific.net/MSF.591-593.514

[8] T.A.G. Restivo, S.R.H. Mello-Castanho. Journal of Power Sources Vol. 185 (2008), p. 1262–1266
doi:10.1016/j.jpowsour.2008.08.082

[9] O. T. Sorensen. J. Thermal Analysis, vol. 38 (1992) 213-228
doi:10.1007/BF02109120

[10] P. L. Husum, O. T. Sorensen. Thermochimica Acta, Vol.114 (1987), P. 131-138
doi:10.1016/0040-6031(87)80251-4

[11] C. C. Guedes E Silva, F.M.S. Carvalho, T. A. G. Restivo. Estudo dos Mecanismos de Difusão em Cerâmicas a Base de Alumina. In: 14ª Congresso Brasileiro de Ciência e Engenharia de Materiais, Águas de São Pedro, SP, Brasil (2000)

[12] T.A.G. Restivo, L. Pagano Jr. Sintering studies on the UO2.Gd2O3 system using SID method, In: Conference on Characterization And Quality Control Of Nuclear Fuels 2002,

Hyderabad, India (2003)

[13] T.A.G. Restivo, L. Pagano Jr. Effect Of Additives On The Sintering Kinetics Of The UO2.Gd2O3 System, In: TCM Brussels, (2003)

[14] M. El Sayed Ali, O.T. Sorensen. Riso-R-518 (1985), p. 12